Maximal capacity partial response signaling

Rusek, Fredrik; Anderson, John B

Published in:
Proc., IEEE 2007 Inter. Conf. Communications

DOI:
10.1109/ICC.2007.140

2007

Maximal Capacity Partial Response Signaling

Fredrik Rusek and John B. Anderson
Dept. of Information Technology
Lund University, Lund, Sweden
Email: {fredrikr,anderson}@it.lth.se

***Abstract*— In this paper we investigate partial response signaling (PRS) systems that are intended to operate close to capacity. We show that finding PRS systems with maximal capacity is a rather easy optimization task. We give an alternate way of defining bandwidth for PRS systems based on capacity considerations; this differs considerably from the traditional method based on transmission power. Practical PRS schemes are derived, based on these ideas. Their bit error rate is significantly better than earlier, distance-optimizing schemes.**

I. Introduction

According to Shannon's classical result, an AWGN channel bandlimited to W positive Hz can support data rates up to $W\log_2(1+P/WN_0)$ bits per second where $N_0/2$ is the noise spectral density and P is the input signaling power. Over the years a major research effort has gone into finding practical coding schemes that approach this limit. However, for single carrier systems, achieving the limit carries with it at least two practical difficulties, Gaussian input alphabet and use of a sinc pulse. Usually a finite input alphabet and non-ideal transmitter pulses are assumed. This implies that many of the best coded modulation schemes today are still bounded well away from Shannon's capacity formula. For example, turbo trellis coded modulation (TTCM), bit interleaved coded modulation and other similar systems are all 1–3 dB away from the capacity that applies to non ideal pulse shapes ($C_1(H)$ to be defined in Section III-C).

When P grows in Shannon's formula, the bit rate R, and consequently the spectral efficiency R/W bits/Hz/s, can be increased. The traditional method of accomplishing this is by expanding the signaling alphabet, thus increasing R. This method is by far the most common in literature as well as in practice. But there exist other methods as well. A class of methods is partial response signaling (PRS). Systems within this class work by introducing a controlled amount of inter-symbol interference (ISI). Its purpose is to achieve a correlated signal in order to reduce bandwidth, i.e., W is reduced but R is constant. Recently, it has been demonstrated that a method called faster than Nyquist (FTN) signaling, which belongs to the PRS class, can have fundamental advantages over its main competitior, Nyquist signaling, since its information rate can be significantly higher [1].

Let b_n be the nth symbol in row vector $\boldsymbol{b} = \ldots, b_{-1}, b_0, b_1, \ldots$. In this paper we consider PRS signals of the form

$$s_{\boldsymbol{a}}(t) = \sqrt{\frac{E_s}{T}} \sum_{k=-\infty}^{\infty} a_k h(t-kT) \tag{1}$$

in which $\boldsymbol{a}$ is a set of data symbols drawn from an alphabet with unit average energy, E_s is the average symbol energy. The pulse $h(t)$ is represented as

$$h(t) = \sum_{l=0}^{L-1} b_l \psi(t-lT) \tag{2}$$

where $\psi(t)$ is any unit energy T-orthogonal pulse shape and $\boldsymbol{b} = b_0, \ldots, b_{L-1}$ is a vector of real valued coefficients with unit energy, i.e. $\boldsymbol{b}\boldsymbol{b}' = 1$. The objective in this and previous papers is to optimize the pulse shape $h(t)$ subject to a bandwidth constraint. Most often the objective function has been the system's minimum distance $d^2_{\min}$. This problem was attacked already in 1974 by Fredriksson [2]; subsequent work appears for example in [3] and [4]. However, the problem was finally solved by Said [5] in 1998 with his development of optimal distance PRS (ODPRS).

Perhaps more important than $d^2_{\min}$ is the bit error rate (BER). Normally it is assumed that the pulse shape maximizing $d^2_{\min}$ will also minimize the BER for high SNRs, but that is not true for ODPRS. The multiplicity of the $d^2_{\min}$-achieving error event is usually so small that it will not be the dominating error event. Since there is no simple expression for the BER the objective function in [6] was selected as the (Forney) union bound. The outcome of that paper was pulse shapes of the same type as ODPRS but with better BER; the gain was typically 0.2–0.5 dB at BER 10^{-5}. This type of PRS is refered to as optimal BER PRS (OBPRS). Both ODPRS and OBPRS are designed for the high energy/low bandwidth region and operate relatively far from capacity. In this paper we will focus on PRS systems that operate closer to capacity, and we will demonstrate that neither distance nor BER are proper objective functions.

II. Basic Properties of PRS Signaling

A. Optimization constraints

Assume that signals are generated according to (1) and (2). Also assume equiprobable binary i.i.d. data symbols $\boldsymbol{a}$.

Let $\boldsymbol{g}$ denote the autocorrelation of $\boldsymbol{b}$, i.e.

$$g_k = \sum_{l=0}^{L-1} b_l b_{l+k}. \tag{3}$$

We can use $\boldsymbol{g}$ to normalize the energy of $h(t)$:

$$\int_{-\infty}^{\infty} |h(t)|^2 dt = g_0 = 1. \tag{4}$$

It is well known that the power spectral density (PSD) of the transmission signal equals $E_s|H(f)|^2/T$. This PSD is a linear function of $\boldsymbol{g}$:

$$\begin{aligned} |H(f)|^2 &= \sum_{k=0}^{L-1} \Psi(f) b_k e^{-i2\pi fkT} \sum_{l=0}^{L-1} \Psi^*(f) b_l e^{i2\pi flT} \\ &= |\Psi(f)|^2 \sum_{k=0}^{L-1} \sum_{l=0}^{L-1} b_k b_l e^{i2\pi f(l-k)T} \\ &= |\Psi(f)|^2 \sum_{k=-(L-1)}^{L-1} g_k e^{i2\pi fkT}. \end{aligned} \tag{5}$$

Traditionally, bandwidth is defined via the spectral power concentration (SPC)

$$\mathcal{C}_h(W) = \frac{\int_{-W}^{W} |H(f)|^2 df}{\int_{-\infty}^{\infty} |H(f)|^2 df} = \int_{-W}^{W} |H(f)|^2 df \tag{6}$$

A fraction $\mathcal{C}_h(W)$ of the transmission power is inside W Hz. Carrying out the integral in (6) yields

$$\mathcal{C}_h(W) = \sum_{n=-(L-1)}^{L-1} g_n \chi_n \tag{7}$$

where $\chi_n \doteq \int_{-W}^{W} |\Psi(f)|^2 e^{i2\pi nfT} df$.

Up to now we have shown that when searching for some sort of optimal PRS system, energy (4) and bandwidth (7) are linear functions of the autocorrelation $\boldsymbol{g}$. However, we must constrain $\boldsymbol{g}$ to be a valid autocorrelation sequence, i.e. there must exist a tap set $\boldsymbol{b}$ that has $\boldsymbol{g}$ as autocorrelation. The following infinite set of linear constraints on $\boldsymbol{g}$ ensures that a tap set $\boldsymbol{b}$ exists:

$$\sum_{n=-(L-1)}^{L-1} g_n \kappa_n(f) \geq 0, \quad \forall f \in [0,1) \tag{8}$$

where $\kappa_n(f) \doteq e^{-j2\pi nf}$. We now state the optimization problem considered in this paper for an arbitrary objective function Γ:

$$\begin{aligned} \boldsymbol{g}_{\text{opt}} &= \arg\max_{\boldsymbol{g}} \quad \Gamma(\boldsymbol{g}) \\ s.t. \quad & \begin{cases} g_0 &= 1 \\ \boldsymbol{g}\boldsymbol{\chi}' &= \mathcal{C}_h(W) \\ \boldsymbol{g}\boldsymbol{\kappa}'(f) &\geq 0 \quad \forall f \in [0,1) \end{cases} \end{aligned} \tag{9}$$

B. Detection

The channel in this paper is assumed to be the AWGN channel with one sided PSD $N_0/2$; the signal at the input to the decoder then becomes $r(t) = s_{\boldsymbol{a}}(t) + n(t)$. Forney has shown [7] that a set of sufficient statistics to estimate $\boldsymbol{a}$ is the sequence

$$y_n = \int_{-\infty}^{\infty} r(t) h(t - nT) dt. \tag{10}$$

Inserting the expression for $r(t)$ into (10) yields

$$y_n = \sum_{n=-\infty}^{\infty} a_n g_{m-n} + \eta_n \tag{11}$$

where g_{m-n} is defined in (3) and

$$\eta_n = \int_{-\infty}^{\infty} n(t) h(t - nT) dt. \tag{12}$$

The receiver model (11) is the so called Ungerboeck observation model. The autocorrelation of the noise sequence $\boldsymbol{\eta}$ is

$$\mathcal{E}\{\eta_n \eta_m\} = \frac{N_0}{2} g_{n-m} \tag{13}$$

Some form of detector should now try to recover $\boldsymbol{a}$ from $\boldsymbol{y}$ in (11). When a MAP detector is used a non-standard approach must be taken; the non-causality of the ISI and the colored noise prohibits the standard BCJR equalizer. But, in a recent paper [8] a BCJR-type algorithm for the Ungerboeck observation model was derived.

III. PRS Optimization

We now present three different PRS objective functions to optimize. Two of them, minimum distance and BER, have been investigated in other papers but for completeness we briefly review them. The third objective function is, to the best of our knowledge, novel.

A. Minimum distance approach (ODPRS)

Optimization of $d^2_{\min}$ of a PRS system with given input alphabet has a long history. It was more or less closed when Said [5] derived a linear theory of optimal PRS codes. Since the codes have maximal $d^2_{\min}$ they have optimal BER as SNR $\rightarrow \infty$. For low SNRs there is no reason to believe that the ODPRS class is optimal since minimum distance plays little role there.

B. BER approach (OBPRS)

When setting $\Gamma(\boldsymbol{g})$ in (9) equal to the BER of an uncoded PRS system, better systems are possible since BER is what one is really after. The problem is that there is no simple expression for BER. However, for moderate or high SNR the well known union bound can be used since it is then tight. It is easy to show that the union bound is convex, which simplifies the optimization. Unlike ODPRS, the OBPRS class is attractive also for low SNR, but then there is no good objective function to use.

C. Maximum capacity PRS (OCPRS)

The third objective function is capacity related. On the most basic level, capacity is defined for the underlying AWGN channel. But equations (1)-(2) can be thought of as defining another channel, whose capacity is not the same. Beyond this, the signals in either of these can be constrained; for example the inputs to either channel can be required to be i.i.d. binary. The limit to the rate of coded systems is then less. We will call such a limit an information rate, under the constraint.

Unfortunately, optimization of PRS information rates is not tractable since there does not exist a closed form expression for the information rate of ISI channels. In [9] lower and upper bounds are given and in [10] a conjectured bound is given that is remarkably tight. Today, accurate simulation based methods to find the information rate are mostly used [11], [12]. But they are not suitable in an optimization because function evaluation is too costly. Capacity is in fact easily computed. This paper seeks PRS systems with maximum capacity. Whether the system bounds itself away from capacity by using a specific input alphabet is of interest but is not addressed here.

We consider objective functions related to two capacities; we then argue that for the cases of interest, the two functions are virtually equivalent. By manipulation of Shannon's formula it is easy to show that signals with PSD shape $E_s/T|H(f)|^2$ in AWGN can only support data rates R (bit/s) satisfying

$$R \le C_1(H) \doteq \int_0^\infty \log_2\Big[1+\frac{2E_s|H(f)|^2}{N_0T}\Big]df. \qquad (14)$$

This is the first objective function. The second relates to (1)-(2). From [9] signals of form (1) can only support data rates up to

$$C_2(H) \doteq \frac{1}{T}\int_0^{1/2} \log_2\Big[1+\frac{2E_s|B(f)|^2}{N_0T}\Big]df \qquad (15)$$

where $B(f)=\sum_{k=0}^{L-1} b_k e^{i2\pi kf}$ is the Fourier transform of $\boldsymbol{b}$.

Capacity $C_1(H)$ cannot be reached with signals of form (1) if there is excess bandwidth in the system, i.e., if $\Psi(f)$ has support outside of $f=1/(2T)$. (One way to reach $C_1(H)$ is to divide the PSD into small pieces and set up individual sinc-pulse coding schemes for each piece). Despite this fact, $C_1(H)$ still constitutes the absolute limit for systems with PSD $E_s|H(f)|^2/T$ and therefore works as a benchmark for any system with this PSD. If the input process is Gaussian with correlation $\boldsymbol{g}$ it is possible to approach $C_2(H)$ [9]. We have therefore proven

Lemma 1:

$$C_1(H) \ge C_2(H). \qquad (16)$$

The cases we are interested in are those with significant bandwidth reduction, i.e. $W<1/(2T)$ with spectral power concentration $\mathcal{C}_h(W)$ very close to 1. If $\Psi(f)$ is flat for $f\in[0,W)$ then $H(f/T)\approx B(f),\ f<1/2$, and $H(f/T)\approx 0,\ f>1/2$. Inspecting (14) and (15) shows that $C_1(H)\approx C_2(H)$ in this case and either of the two can be used. In the sequel we use $C_2(H)$.

Next we prove

Lemma 2: $C_2(H)$ is a convex function of $\boldsymbol{g}$.

Proof Let $\alpha_n(f)=e^{i2\pi nfT}$ and $\boldsymbol{\alpha}(f)$ be the row vector formed from $\alpha_n(f),\ -(L-1)\le n\le L-1$. Then $|B(f)|^2$ in (15) can be written as

$$|B(f)|^2 = \boldsymbol{g}\boldsymbol{\alpha}'(f). \qquad (17)$$

To simplify notation, write

$$C_2(\boldsymbol{g}) \doteq C_2(\boldsymbol{g}\boldsymbol{\alpha}'(f)) = C_2(H). \qquad (18)$$

Evaluating $TC_2(\lambda\boldsymbol{g}_1+(1-\lambda)\boldsymbol{g}_2)$ gives

$$\begin{aligned} TC_2(\lambda\boldsymbol{g}_1+(1-\lambda)\boldsymbol{g}_2) &= \int_0^{1/2}\log_2\Big[1+2\frac{[\lambda\boldsymbol{g}_1+(1-\lambda)\boldsymbol{g}_2]\boldsymbol{\alpha}'(f)}{N_0T}\Big]df \\ &= \int_0^{1/2}\log_2\Big[\lambda+(1-\lambda)+ \\ &\quad +2\frac{\lambda\boldsymbol{g_1}\boldsymbol{\alpha}'(f)+(1-\lambda)\boldsymbol{g}_2\boldsymbol{\alpha}'(f)}{N_0T}\Big]df \\ &= \int_0^{1/2}\log_2\Big[\lambda(1+2\frac{\boldsymbol{g}_1\boldsymbol{\alpha}'(f)}{N_0T})+ \\ &\quad +(1-\lambda)(1+2\frac{\boldsymbol{g}_2\boldsymbol{\alpha}'(f)}{N_0T}\Big]df. \end{aligned} \qquad (19)$$

The logarithm is convex, so we obtain

$$C_2(\lambda\boldsymbol{g}_1+(1-\lambda)\boldsymbol{g}_2) \ge \lambda C_2(\boldsymbol{g}_1)+(1-\lambda)C_2(\boldsymbol{g}_2) \qquad (20)$$

and the proof is complete. ■

By variational calculus it can be shown that (15) is maximized by the pulse shape

$$|H_{\max}(f)|^2 = \begin{cases} \mathcal{C}_h(W)/(2WT), & |f|\le WT \\ (1-\mathcal{C}_h(W))/(1-2WT), & WT\le|f|\le 1/2 \\ 0, & \text{otherwise} \end{cases} \qquad (21)$$

where $\mathcal{C}_h(W)$ is the SPC constraint. Inserting (21) into (15) gives

$$\begin{aligned} C_2(H_{\max}) = \frac{1}{T}\Big[&WT\log_2(1+\frac{E_s}{N_0}\frac{\mathcal{C}_h(W)}{WT})+ \\ &+(\frac{1}{2}-WT)\log_2(1+\frac{E_s}{N_0}\frac{1-\mathcal{C}_h(W)}{1/2-WT})\Big] \end{aligned} \qquad (22)$$

The first term of (22) is the capacity contribution from the passband and the second term is the contribution from spectrum outside the nominal bandwidth W. It can be seen that when $WT\to 0$ we must let $\mathcal{C}_h(W)\to 1$ if the first term is to dominate (22). When the second term starts to grow it means that a considerable amount of the information is transmitted in the stopband. The second term is denoted *out-of-band capacity*. It gives a quality measure on $\mathcal{C}_h(W)$; when there is too much out of band capacity the nominal bandwidth W should not be considered as the signal bandwidth.

Therefore, we propose to design PRS systems by limiting the out-of-band capacity instead of the out-of-band power. We start by defining the *capacity concentration* function as

$$\Theta(WT,\mathcal{C}_h(W),E_s/N_0) = \frac{\frac{1}{T}WT\log_2(1+\frac{E_s}{N_0}\frac{\mathcal{C}_h(W)}{WT})}{C_2(H_{\max})}. \qquad (23)$$

This is the first term of (22) divided by the whole expression (22), i.e., the relative amount of capacity located inside W Hz for the optimal pulse. When there can be no confusion we will refer to $\Theta(WT,\mathcal{C}_h(W),E_s/N_0)$ as Θ only. We will define bandwidth as the frequency where Θ reaches a certain value, such as .999.

An investigation of Θ in detail is important, but it is beyond the scope of this paper. We give some facts as a lemma; the proofs are simple exercises with limits.

Lemma 3:

$$\Theta(WT, \mathcal{C}_h(W), E_s/N_0) \to \begin{cases} \mathcal{C}_h(W) & E_s/N_0 \to 0 \\ 2WT & E_s/N_0 \to \infty \\ 0 & WT \to 0 \end{cases} \tag{24}$$

It is assumed that $\mathcal{C}_h(W) < 1$ for the two last limits. The first limit implies that for poor channels there is no difference between the spectral power and capacity concentration. The second limit basically prohibits PRS systems from operating at high energy, as most of the capacity then lies outside the nominal bandwidth. The third limit prohibits too much bandwidth reduction.

Moreover, for almost all combinations of $\{WT, \mathcal{C}_h(W)\}$, Θ is a monotonically decreasing function for increasing E_s/N_0; but for some setups, especially when $\mathcal{C}_h(W)$ is small, Θ can grow for increasing E_s/N_0. When Θ decreases for increasing E_s/N_0 it usually decreases rapidly, making the spectral power concentration useless as a bandwidth measure.

We give an example of the difference between the capacity and spectral power concentrations. In [5, Fig. 6] an ODPRS system based on 4 PAM is proposed. System parameters are $WT = 0.2$, $E_s/N_0 = 28$dB and $\mathcal{C}_h(W) = .999$. This scheme seems to achieve an impressive 12 dB gain over uncoded QAM. But examining $\Theta(WT, \mathcal{C}_h(W), E_s/N_0)$ reveals that only 83 % of the capacity is located inside W Hz. In order to signal efficiently with PRS systems in this low bandwidth/high energy region a much higher value for the spectral power concentration must be used in the design.

It should be pointed out that bandwidth measures based on the capacity concentration do not tell us anything about disturbance to frequency bands outside $[-W, W]$. To measure this we must still use spectral power concentration. Moreover, the capacity concentration idea is based on the optimal pulse shape and a coding scheme that approaches capacity; thus, it gives only rough insight into systems with non-ideal pulse shape and coding.

The capacity concentration can also be used to estimate performance in situations where there is interference in the stopband. Assume that $C_2(H_{\max})$ bit/s are transmitted error free and that the stopband suddenly vanishes. Standard rate-distortion theory states that the BER must be larger than β, where β satisfies

$$\Theta(WT, \mathcal{C}_h(W), E_s/N_0) = 1 - h_b(\beta), \tag{25}$$

where $h_b(\ )$ is the binary entropy function. Evaluating (25) for $\Theta = .999$ gives $\beta = 6 \times 10^{-5}$; if smaller BER are desired Θ must be increased. Evaluating (25) for the example ODPRS system in [5] gives $\beta = 2.5 \times 10^{-2}$; thus WT can definitely not be regarded as the bandwidth for that parameter setup.

When optimizing over a finite L taps we have already shown that the objective function is convex. Since the domain is given by linear constraints, the domain is also convex. Moreover, the domain is compact and the objective function is continuous, which implies that the optimization problem indeed has a solution. When performing the optimization we have used the routine *fmincon.m* in MATLAB. It should be pointed out that the capacity optimization is considerably easier than the BER or distance optimizations as it has fewer constraints [5], [6].

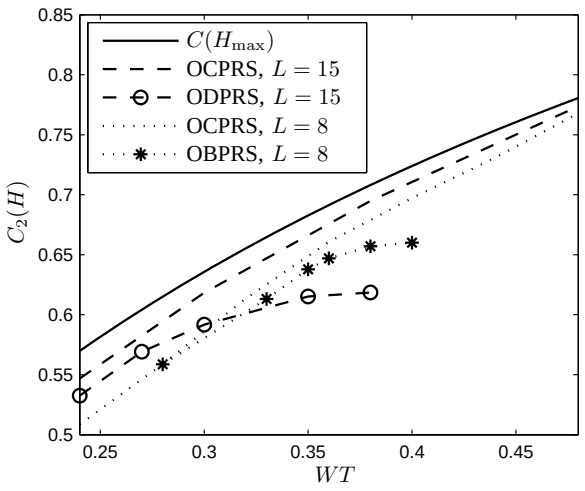

Fig. 1. Outcome of the capacity optimization plotted against WT, for $\mathcal{C}_h(W) = .999$. $C(H_{\max})$ is included for comparison.

In Figure 1 we show some results of this optimization and how they compare to the ODPRS and OBPRS classes. We plot capacity $C(H)$ versus the nominal bandwidth WT based on spectral power, where $\mathcal{C}_h(W) = .999$ in all cases. The cases $L = 8$ and $L = 15$ are plotted. Also shown is $C_2(H_{\max})$, which is an upper bound. As the number of taps increases the OCPRS approaches $C_2(H_{\max})$, i.e. the optimization tries to create a pulse with a brickwall spectrum. The OCPRS has higher capacity than both OBPRS and ODPRS, but as the nominal bandwidth decreases the gap gets smaller. For $L = 8$ and $WT = .28$ the gap actually closes. This happens because the bandwidth constraint gets more restrictive and the domain gets smaller, and consequently there is not much freedom when optimizing the pulse shape. The most striking result is that as WT grows the capacity of the OBPRS and ODPRS classes start to flatten out. When computing the capacities in Figure 1 we used $E_s/N_0 = 1$; the outcome of the optimization will of course change when E_s/N_0 is changed. Moreover, due to the low value of E_s/N_0 in Figure 1, the capacity concentration is by Lemma 3 close to $\mathcal{C}_h(W)$ (it is always above .9975).

IV. Some Concatenated Coding Schemes

Even if OCPRS has higher capacity than ODPRS, it is not certain that coding schemes where PRS is used as modulation will perform better when OCPRS is used. To analyze this, we calculate some EXIT charts for the PRS systems. Recall that if system A has an EXIT curve that is strictly higher than

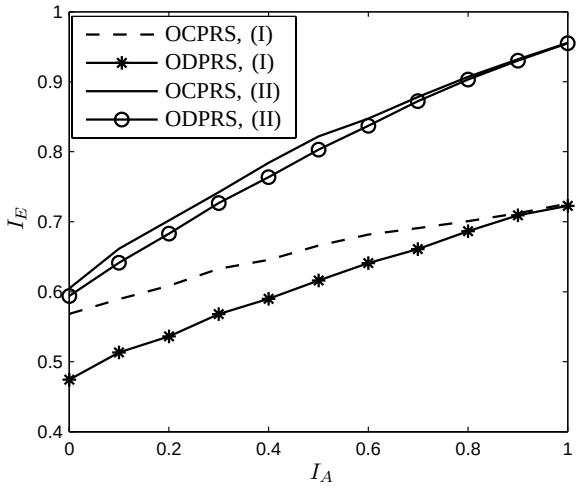

Fig. 2. EXIT curves for two parameter setups. For both setups the EXIT curves for both OCPRS and ODPRS are plotted.

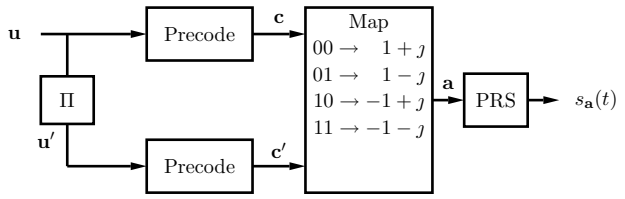

Fig. 3. System model for the parallel coding scheme. $\jmath$ denotes the imaginary unit. The PRS block implements (1)-(2).

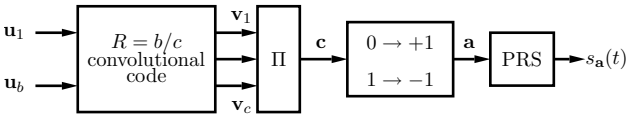

Fig. 4. System model for serial concatenation. The PRS block implements (1)-(2).

system B, then system A will converge at lower SNR and thus is more suitable for iterative decoding. By standard arguments it is also plausible that system A has higher information rate than system B. For more about EXIT charts see [13].

In Figure 2 we show EXIT charts of both OCPRS and ODPRS for two parameter setups. For both we use $L = 6$ and $\mathcal{C}_h(W) = .999$. For the first setup (I) we use $WT = .40$ and $E_s/N_0 = 0$ dB. For the second setup (II) we use $WT = .30$ and $E_s/N_0 = 4$ dB. From the curves it is seen that the OCPRS systems have considerably better EXIT curves and we therefore expect much better performance from them. As we would expect from Figure 1, OCPRS and ODPRS differ more when WT is large (system I); for the smaller $WT = .30$ the ISI responses $\boldsymbol{b}$ are quite similar for OCPRS and ODPRS. EXIT curves for OBPRS lie in between those of ODPRS and OCPRS.

A problem that arises is that the decoding complexity grows exponentially with the number of ISI taps L. This effectively prohibits L larger than $6 - 8$ for binary signaling. However, an interesting result is that if the PRS code $\boldsymbol{b}$ is designed for, e.g., 15 taps, but the decoder only considers, say, the first 6 taps of $\boldsymbol{b}$, the EXIT curves of the truncated decoder are often still above those of a PRS code designed with 6 taps. The taps not considered by the decoder act as noise; if there are many ignored taps the noise is approximately Gaussian. But these ignored taps will help the transmitter to create a pulse satisfying the bandwidth criteria.

There exists an interesting connection between the reduced complexity detection of PRS and the faster than Nyquist (FTN) signaling mentioned in Section I. An FTN system can sometimes be seen as a PRS system with system model as in (1) but with infinite length, i.e., $L = \infty$, and 100 % spectral power concentration, $\mathcal{C}_h(W) = 1$. Clearly, an FTN scheme cannot be decoded with full MAP/MLSE decoding as the complexity would be infinite. Yet, in [1] there are examples of coding schemes based on FTN that outperform the information rates of coding schemes built on 8 PSK and 16 QAM signals.

Next, we construct tentative coding schemes where the PRS system is used as the inner encoder. We wish to find out whether OCPRS indeed outperforms ODPRS and OBPRS. The first coding structure is shown in Figure 3. A bit sequence $\boldsymbol{u}$ is to be transmitted. The sequence is first interleaved to produce the sequence $\boldsymbol{u}^{\,prime}$. The two sequences are then precoded by a recursive precoder which produces the sequences $\boldsymbol{c}$ and $\boldsymbol{c}'$. These two are then transmitted by two independent PRS systems with independent AWGN, here taken as an I/Q QPSK scheme. The recursive precoder used in Figure 3 works as follows. Output bit c_k is formed as

$$c_k = u_k \prod_{l=1}^{N} c_{k-l}\nu_l \tag{26}$$

where the coefficients $\nu_k, \quad 1 \leq k \leq N$, $\nu_k \in \{0, 1\}$, completely characterize the precoder. When $N \leq L$ no additional decoding complexity is added by the precoder.

The EXIT curves in Figure 2 do not have the property that $I_E = 1$ for $I_A = 1$. This property is however crucial; it is easy to see that the coding scheme in Figure 3 completely fails if this is not satisfied. But the precoder transforms the EXIT curves such that $I_E = 1$ for $I_A = 1$ regardless of the SNR. This comes with a penalty for lower SNRs where the new curves fall below the non-precoded curves. The system will converge when the EXIT curve is above the line $I_E = I_A$.

The second structure is shown in Figure 4. A bit sequence $\boldsymbol{u}$ is encoded with a convolutional code of rate b/c. An interleaver and BPSK mapping follows and finally PRS modulation. Decoding is done by ordinary turbo equalization. For more details on the coding schemes and decoding of them we refer to [14].

Simulations of the parallel system in Figure 3 are shown in Figure 5. System parameters are $WT = .40$, $L = 6$, $\mathcal{C}_h(W) = .999$, and the interleaver blocksize is 10000. The precoder has $\nu_k = 1, \ 1 \leq k \leq 5$. We tested all three classes of PRS.

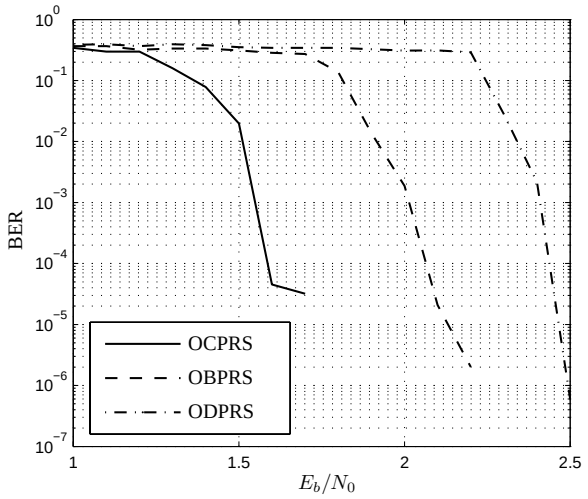

Fig. 5. Simulations of the parallel concatenated scheme. System parameters are $L = 6$, $WT = .35$ and $\mathcal{C}_h(W) = .999$.

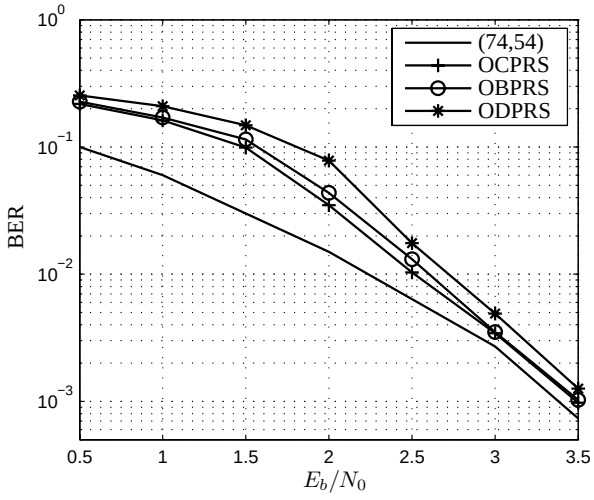

Fig. 6. Simulations for a serial concatenated scheme. Outer encoder is the (74,54) convolutional code, random interleaver with blocklength 2048 and a 6 tap PRS modulator with $WT = .35$ and $\mathcal{C}_h(W) = .999$.

It can be seen that the OCPRS class performs much better than the other two. We believe that this is due to its superior capacity, which the system operates relatively near. Moreover, since WT is quite large and E_b/N_0 is small we expect a large value for Θ and thus the bandwidth measure is considered appropriate. For E_b/N_0 =1.6 dB the actual value for Θ is .9983. We consider this system setup as a proper use of PRS.

Simulations of the serial system in Figure 4 are shown in Figure 6. It can be shown [14] that the system can never perform better than the underlying convolutional code, in this case the rate $1/2$ convolutional code (74, 54) in octal notation. The performance of the code alone is included in Figure 6. We test all three classes of PRS. System parameters are $WT = .35$, $L = 6$, $\mathcal{C}_h(W) = .999$ and the interleaver blocksize is 2048 bits. It is seen that OCPRS has the smallest BER for a given E_b/N_0. As E_b/N_0 grows all three classes more or less have the same performance. This is natural; as E_b/N_0 grows all possible PRS systems will converge to the convolutional code performance and there is no way to improve that without changing the system. The region where different PRS codes can give different performance is at small E_b/N_0, and there OCPRS is best.

V. Conclusions

We have investigated optimal partial response signaling. We have considered three objective functions, two previously investigated and a new one based on capacity. The outcome is that PRS codes with optimal capacity perform better at low SNRs than other types of optimal PRS. The associated optimization problem is also easier than for other types of optimal PRS. We have introduced the capacity concentration function, which measures the capacity inside the nominal bandwidth. In the low bandwidth/high energy region, where PRS codes are usually intended to operate, there is a major difference between the capacity concentration and the traditional spectral power concentration. The capacity concentration function seems to be very important for PRS.

References

[1] F. Rusek and J.B. Anderson, "On Information Rates of Faster than Nyquist Signaling," *Proc.* Globecom 2006, San Francisco, Nov. 2006.

[2] S.A. Fredricsson, "Optimum Transmitting Filter in Digital PAM Systems with a Viterbi Detector," *IEEE Trans. Information Theory*, IT–20, vol. 479–489, July 1974.

[3] G.J. Foschini, "Contrasting Performance of Faster Binary Signaling with QAM," *AT&T Bell Labs. Tech. J.*, vol. 63, pp 1419–1445, Oct. 1984.

[4] C. W.-C. Wong and J.B. Anderson, "Optimal Short Impulse Response Channels for an MLSE Receiver," *Conf. Rec.*, Intern. Conf. Commun., Boston, 25.3.1–25.3.5, June 1979.

[5] A. Said and J.B. Anderson, "Design of Optimal Signals for Bandwidth-efficient Linear Coded Modulation", *IEEE Trans. Information Theory*, vol. 44, pp. 701–713, March 1998.

[6] F. Rusek and J.B. Anderson, "Near Bit Error Rate Optimal Partial Response Signaling," *Proc.*, 2005 Intern. Symp. Information Theory, Adelaide, Sept 2005.

[7] G. D. Forney, Jr., "Maximum Likelihood Sequence Estimation of Digital Sequences in the Presence of Intersymbol Interference," *IEEE Trans. Information Theory*, IT-18, 363–378, May 1972.

[8] G. Colavolpe and A. Barbieri, "On MAP Symbol Detection for ISI Channels using the Ungerboeck Observation Model", *IEEE Commun. Letters*, vol. 9, Aug. 2005.

[9] S. Shamai, L.H. Ozarow and A.D. Wyner, "Information Rates for a Discrete-Time Gaussian Channel with Intersymbol Interference and Stationary Inputs," *IEEE Trans. Information Theory*, vol. 37, pp. 1527–1539, Nov. 1991.

[10] S. Shamai and R. Laroia, "The Intersymbol Interference Channel: Lower Bounds on Capacity and Channel Precoding Loss," *IEEE Trans. Information Theory*, vol. 42, no. 5, pp. 1388–1404, Sept. 1996.

[11] D. Arnold and H.-A. Loeliger, "On the Information Rate of Binary-Input Channels with Memory," *Proc.* Intl. Conf. Commun., Helsinki, June, 2001, pp. 2692–2695.

[12] H. D. Pfister, J. B. Soriaga, and P. H. Siegel, "On the Achievable Information Rates of Finite State ISI Channels," *Proc.* GLOBECOM 2001, San Antonio, TX, vol. 5, Nov. 2001, pp. 2992–2996

[13] S. ten Brink, "Convergence of Iterative Decoding," *IEE Electronics Letters.*, vol. 35, pp. 806–808, May 1999.

[14] F. Rusek and J.B. Anderson, "On Serial and Parallel Concatenations Based on Faster than Nyquist Signaling," *Proc.*, 2006 Intern. Symp. Information Theory, Seattle, July 2006.